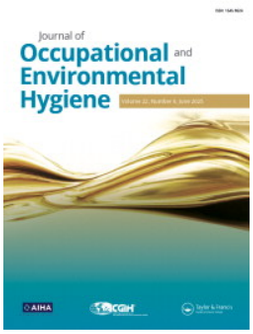

Taylor & Francis
Taylor & Francis Group

Journal of Occupational and Environmental Hygiene

ISSN: 1545-9624 (Print) 1545-9632 (Online) Journal homepage: www.tandfonline.com/journals/uoeh20

Toward rapid silica analysis of CPDM samples: A study of dust recovery and quartz estimation using lab and field samples

August Greth, Garek Elie & Emily Sarver

To cite this article: August Greth, Garek Elie & Emily Sarver (2025) Toward rapid silica analysis of CPDM samples: A study of dust recovery and quartz estimation using lab and field samples, Journal of Occupational and Environmental Hygiene, 22:6, 460-473, DOI: 10.1080/15459624.2025.2471392

To link to this article: https://doi.org/10.1080/15459624.2025.2471392

JOURNAL OF OCCUPATIONAL AND ENVIRONMENTAL HYGIENE
2025, VOL. 22, NO. 6, 460–473
https://doi.org/10.1080/15459624.2025.2471392

Taylor & Francis
Taylor & Francis Group

RESEARCH ARTICLE

Toward rapid silica analysis of CPDM samples: A study of dust recovery and quartz estimation using lab and field samples

August Greth, Garek Elie, and Emily Sarver

Department of Mining and Minerals Engineering, Virginia Polytechnic Institute & State University, Blacksburg, Virginia

ABSTRACT

In US coal mines, the continuous personal dust monitor (CPDM) is frequently used to determine miners' exposure to respirable dust. Capabilities to analyze the respirable crystalline silica (RCS) content of that dust are needed, but the CPDM sample collection substrate ("stub") interferes with direct analysis. To overcome this challenge, a three-step method is proposed to recover the dust from the stub, deposit the dust on a polyvinyl chloride (PVC) filter, and analyze the recovered dust by Fourier Transform Infrared Spectroscopy (FTIR) to determine the quartz content (as a proxy for RCS). Recent work has established procedures for the latter two steps using representative dust samples suspended in isopropyl alcohol (IPA). That work is extended in the current study to also address the dust recovery step, testing both IPA and deionized water (H_2O) as recovery liquids. Here, blank CPDM stubs were subjected to the entire three-step method and results were used to establish a quartz mass correction for residue that is recovered from the stub itself. Then, the method and correction were applied to lab-spiked and field CPDM stubs. For spiked samples, predicted and expected quartz mass values were highly correlated (R^2 values >0.97 regardless of recovery liquid or application of the blank CPDM-stub correction); though predicted values were consistently lower than expected values (regression line slopes between 0.84 and 0.86), which might be related to effects of total recovered sample mass on the deposition pattern achieved on PVC filter. For the field samples, IPA proved to be a much more efficient recovery liquid than H_2O. Unfortunately, the evaluation of the predicted quartz mass results on the field samples was confounded by apparent issues with reference filter samples intended to determine expected values.

KEYWORDS

Continuous personal dust monitor; Fourier transform infrared spectroscopy; respirable coal mine dust; respirable crystalline silica

Introduction

Beginning in the late 1990s, there has been an alarming uptick in the prevalence of Coal Worker's Pneumoconiosis (CWP, or "Black Lung") in the United States (Hall et al. 2019). In Central Appalachia, prevalence of the most severe form of CWP, progressive massive fibrosis (PMF), has been especially high (Blackley et al. 2018; Harris et al. 2024). CWP is caused by overexposure to respirable coal mine dust (RCMD) (Hall et al. 2020; Vanka et al. 2022), which can have a variable composition depending on dust sources and controls in the mining environment. Commonly, though, RCMD includes some amount of respirable crystalline silica (RCS), and this constituent appears to be a key factor driving the recent trends in PMF (Hall et al. 2019; Cohen et al. 2022).

In response to resurgent disease, the Mine Safety and Health Administration (MSHA) published a "new dust rule" in 2014, which reduced the permissible exposure limit (PEL) for RCMD, in total, from 2.0 mg/m^3 to 1.5 mg/m^3 ("Lowering miners' exposure to respirable coal mine dust, including continuous personal dust monitors" 2014). That rule also mandated the use of new monitoring technology called the continuous personal dust monitor (CPDM), which is now required for all mine operator-conducted sampling. Further, MSHA published a "new silica rule" in 2024 to reduce the PEL for RCS, specifically, from an effective limit of 100 $\mu g/m^3$ to 50 $\mu g/m^3$ ("Lowering miners' exposure to respirable crystalline silica and improving respiratory protection" 2024). These limits will apply to all miners and will be measured as an

CONTACT Emily Sarver esarver@vt.edu Department of Mining and Minerals Engineering, Virginia Polytechnic Institute & State University, Blacksburg, Virginia.

Supplemental data for this article can be accessed online at https://doi.org/10.1080/15459624.2025.2471392.
AIHA and ACGIH members may also access supplementary material at http://oeh.tandfonline.com.

8-hr time-weighted average (TWA) based on samples collected throughout a full worked shift. The "new silica rule" also sets an RCS action level at 25 $\mu g/m^3$.

Before the CPDM was required, all respirable dust sampling was done using a Coal Mine Dust Personal Sampling Unit (CMDPSU)—and both mine operators and MSHA collected samples to demonstrate regulatory compliance. The CMDPSU is a traditional filter sampler that collects respirable dust onto a 37 mm polyvinyl chloride (PVC) filter. The filter sample can be (and was historically) used to determine the RCMD concentration by gravimetric analysis. Additionally, it can (and will continue to) be used to determine RCS concentration by Fourier transform infrared spectroscopy (FTIR) using α-quartz as a surrogate analyte (i.e., since α-quartz, herein termed quartz, is the predominant form of RCS in coal mines, see Key-Schwartz et al. (2003)). For compliance samples, the RCS analysis is conducted using the standard MSHA Method P-7 *Infrared Determination of Quartz in Respirable Coal Mine Dust* (Goldberg et al. 1984; "Infrared determination of quartz in respirable coal mine dust (U.S.)" 2013). Briefly, the sample is ashed to remove combustible matter (i.e., coal dust and the PVC filter itself); the residue is deposited onto a new filter; and that filter is analyzed to determine quartz mass, which can be converted to mass concentration knowing the sampling flowrate and duration. However, since MSHA Method P-7 requires substantial sample preparation and must be performed in a certified lab, there are delays between sampling and results reporting—which can complicate efforts to pinpoint and correct factors contributing to overexposures.

Moving forward with the "new silica rule," certified lab analysis of filter samples will still be required to demonstrate RCS regulatory compliance on at least a quarterly basis. However, the ability to collect more data, especially more timely data, could be quite valuable for non-regulatory purposes such as permitting mines to keep an eye on RCS concentrations between compliance measurements, gauge the effects of new dust controls, or monitor changing mining conditions.

To enable more timely RCS data, researchers at the National Institute for Occupational Safety and Health (NIOSH) have developed a standardized method for direct-on-filter (DOF) quartz analysis by FTIR (National Institute for Occupational Safety and Health 2022). It uses the same PVC filter samples as would be collected for the Method P-7 analysis, but no sample preparation is required. Thus, with a portable FTIR instrument, the DOF method can be performed in the field to provide rapid (e.g., end-of-shift) results. Nevertheless, a main challenge to the widespread adoption of the DOF FTIR method is that many coal mines are no longer using—and do not even possess—the CMDPSUs needed for filter sampling. Rather, following the "new dust rule" they have moved almost exclusively to using the CPDM (i.e., with only MSHA collecting filter samples for RCS monitoring). A CPDM is worn by a miner and allows for real-time RCMD concentration monitoring (NASEM 2018). In essence, the instrument continuously samples RCMD and measures the accumulation of the sample mass using an internal microbalance. However, there is currently no analytical method to enable RCS determination in the collected sample.

While FTIR analysis of CPDM samples has previously been considered, a main challenge is the makeup of the CPDM's filter stub assembly, referred to as "filter stub" or simply "stub." It consists of a borosilicate glass fiber and polytetrafluoroethylene (PTFE) filter, with a woven glass backing mounted to a polypropylene (PP) stub (Chow et al. 2022). The glass materials directly interfere with the IR spectral peaks of the target quartz analyte, which prevents typical DOF analysis using IR absorbance or transmission (Tuchman et al. 2008); attempts to use diffuse reflectance IR have also been unsuccessful (Miller et al. 2015). However, a method that includes a simple dust recovery step, followed by deposition of the recovered dust onto a PVC filter might represent a feasible workaround. Figure 1 presents a conceptual illustration of such a method.

To this end, recent work by the authors has focused on the deposition and analysis steps shown in Figure 1 (Greth and Sarver 2025). Starting with representative respirable dust suspensions in isopropyl alcohol (IPA), that work determined a simple syringe filter apparatus (i.e., 50-mL syringe with Luer Lock connection to an in-line PP syringe filter holder) can be used to deposit the dust onto a blank 25 mm PVC filter—with a characteristic deposition pattern that is repeatable (i.e., same pattern on each filter). Once dry, the loaded filter can be scanned by FTIR, and quartz mass can be derived from the resulting spectrum. This is essentially the same way that quartz mass is determined via NIOSH's DOF method, except that the location of FTIR analysis on the filter is changed. For NIOSH's DOF method (i.e., 37 mm PVC filters with RCMD collected directly from the mine atmosphere), a single scan in the filter's center is used (National Institute for Occupational Safety and Health 2022). However, the authors' previous work (i.e., 25 mm PVC filters with dust deposited from suspension)

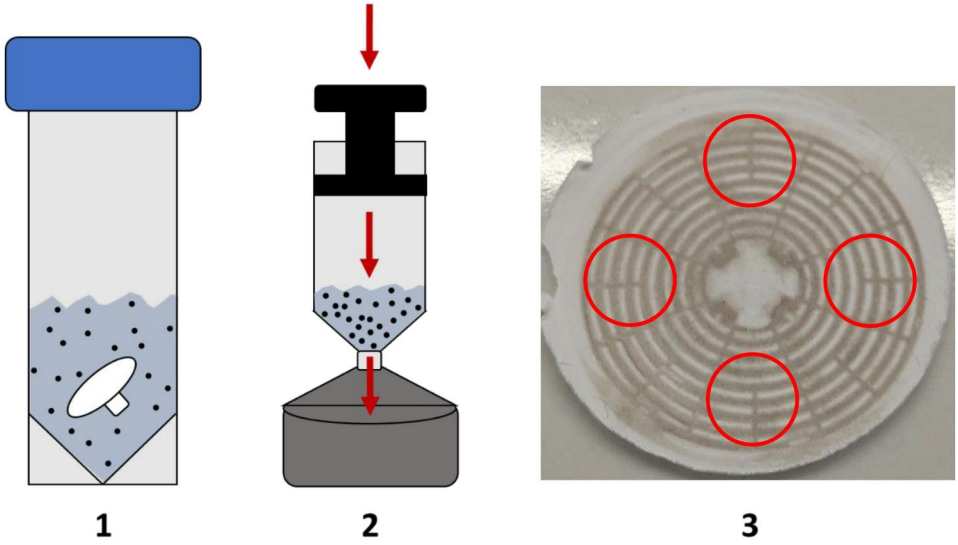

Figure 1. Conceptual illustration of a method to enable FTIR analysis of CPDM samples, wherein (1) dust is recovered into a suspension from the CPDM filter stub; (2) the recovered dust is deposited onto a clean PVC filter; and (3) the PVC filter is analyzed by FTIR using preset scan locations.

established a procedure for scanning the filter at four points (each offset from the filter center by 8 mm, 90° apart) and averaging the results (Greth and Sarver 2025) This was based on the characteristic deposition pattern yielded by the in-line PP filter holder (see Figure 1).

Though the previous work addressed deposition and FTIR analysis of recovered dust, it did not address the actual recovery procedure—nor the possible sample contamination that might result from the CPDM filter assembly, referred to as "CPDM stub" or simply "stub," itself. These are the subjects of the current study. Here, a simple recovery procedure was tested which involved shaking the CPDM stub in a liquid to create a dust suspension; and then the dust was deposited from the suspension and analyzed using the previously established procedures (i.e., per Figure 1, and as detailed in Greth and Sarver 2025). Experiments were conducted in three phases with three different sample types: (1) samples generated from blank CPDM stubs ("blank CPDM"), which were used to observe the range of residue that might be expected from the filter stubs themselves and to establish corrections for their contribution to total sample mass and quartz mass; (2) samples generated from blank CPDM stubs spiked with respirable dust of known quartz content ("spiked CPDM"), which were used to test the CPDM stub residue corrections; and (3) samples generated from real CPDM stubs collected in the field ("field CPDM"), which were used to evaluate the three-step method shown in Figure 1 by comparison to reference quartz analysis on paired CMDPSU filter samples. Notably, within all three phases, experiments were conducted using both IPA and deionized water ("H_2O") as the recovery liquid. The previous work used IPA due to its rapid evaporation rate and because it is well-established for methods requiring particle recovery/resuspension procedures (Goldberg et al. 1984; Ainsworth 2005; Agioutanti et al. 2020). However, H_2O was also tested here as an alternative recovery liquid for a possible field-based method. It is readily available and presents minimal contamination potential, and effectively no safety risk.

Materials and methods

Blank CPDM filter stub samples

A total of 40 samples were prepared from blank CPDM stubs (Thermo Scientific, Waltham, MA). For this, clean stainless steel tweezers were used to transfer a stub into a clean 50 mL test tube, and then either 5 mL of IPA ($n = 20$) or H_2O ($n = 20$) was added to completely submerge the stub. Care was taken not to touch the borosilicate filter surface during handling (i.e., the tweezers gripped the PP stub frame). Test tubes were capped and placed into a test tube holder that was secured to a shaker table (Thermolyne Bigger Bill, Dubuque, Iowa, USA) using zip ties, and the shaker was turned on for 1 min at 350 RPM. The test tubes were then uncapped, and the stubs were carefully removed. Then, the tubes were recapped to minimize evaporation before each suspension could be filtered (i.e., to deposit any particulate recovered from the CPDM stub).

Suspensions were filtered through 25 mm PVC filters (Zefon International, Ocala, FL, USA), which were pre-

weighed using a Cubis MSE6.6S microbalance (Sartorius, Gottingen, Germany). After pre-weighing, each filter was loaded into a PP in-line syringe filter holder (Sterlitech Corporation, Auburn, WA) along with a cellulose backing pad. The filter holders have Luer Lock inlets and were used with 50 mL sterile syringes (BD, Franklin Lakes, NJ). After the suspension was pushed through the PVC filter, the holder was opened, and the filter was carefully transferred to a two-piece cassette (inlet and outlet plugs removed) and allowed to dry completely in a clean fume hood for at least 12 hr. Then it was re-weighed and sample mass (M, mg) was determined using Equation 1:

$$M = F_2 - F_1 \quad (1)$$

where F_1 and F_2 are the filter pre- and post-weights, respectively. Greth and Sarver (2025) previously investigated this method for deposition of dust from a suspension in IPA, followed by quartz analysis. In that work, dust samples deposited onto 25 mm PVC filters were weighed and handled (for analysis) during three consecutive events, and negligible changes in sample mass were observed.

Spiked CPDM filter stub samples

Another 40 samples were prepared using blank CPDM stubs spiked with respirable-sized dust of known quartz content. These samples were prepared using the same procedure described above to shake a blank stub in either IPA ($n = 20$) or H_2O ($n = 20$); however, this time, after the stub was removed from the test tube, a small mass of respirable dust from one of two sources was added to the tube to create a suspension that included any residue from the stub as well as dust particles.

The respirable dust was collected from one of two bulk samples of material representing a real source of coal mine dust. One material was "bolter dust," which was taken directly from the dust collection system of a roof bolter machine at a partner mine; and the other was created from raw "roof rock" that was taken from the production belt in a different partner mine. To create the dust source material from the roof raw, large pieces of the rock (i.e., between 20 and 100 cm) were pulverized and sieved to yield a top size of approximately 60 µm. Respirable dust from both source materials was previously analyzed by the standard NIOSH Method 7603 *QUARTZ in Coal Mine Dust, by IR (redeposition)* to determine quartz content, and results showed the bolter dust contained an average of 9.51% quartz and the roof rock contained 10.5% quartz based on the results of two samples for each dust type. For this study, respirable dust was collected from each materials using the following procedure: A small mass of the material was placed in an enclosure and aerosolized using compressed air, and CMDPSUs (i.e., 10 mm nylon cyclone with a personal air pump at 2.0 L/min) were used to collect the respirable dust directly onto 37 mm polytetrafluoroethylene (PTFE) filters (Zefon International, Ocala, FL, USA) in closed two-piece cassettes. The PTFE filters were pre- and post-weighed to estimate the total mass of respirable dust collected, and a total of 20 filters were collected for each material having mass in the range of about 0.1 to 2.0 mg to simulate realistic CPDM sample masses that might be expected in the field.

To add the coal mine source dust to each suspension (i.e., already containing any residue from a blank CPDM stub), one of the loaded PTFE filters was submerged in the test tube; this was done to create 10 samples representing each recovery liquid and dust source combination (i.e., $n = 10$ for bolter dust in IPA, $n = 10$ for roof rock with IPA, $n = 10$ for bolter dust with H_2O, and $n = 10$ for roof rock with H_2O). Next, the tubes were capped and placed into a sonic bath at 32 °C for 3 min to dislodge the dust from the PTFE filters. Then, the PTFE filters were removed from the tubes and the tubes were recapped until the suspensions were deposited onto pre-weighed 25 mm PVC filters (i.e., using the same procedure described above.) Finally, the dry PVC filters were re-weighed such that sample mass could be determined using Equation 1.

Field CPDM and reference samples

A total of 34 samples were prepared from CPDM stubs that were collected as part of a separate study (Elie et al. 2024) and leveraged for the current work (see Supplementary material, Table S1). Importantly, as part of the mine sampling to collect the CPDM stubs, CMDPSUs were also used to collect paired PVC filter samples which could be utilized for reference analysis.

Mine sampling

The CPDM stubs and paired PVC filter samples were collected in an underground room and pillar mine. Field sampling was conducted during 20 separate sampling events, representing a fixed location during a particular production shift. The locations were expected to have relatively high dust concentrations (i.e., just downwind of an active continuous miner or roof bolter, or in the return airway of the mine section). In all, two CPDM stubs were available from

each of 14 events and a single CPDM stub was available from each of the other six events (i.e., 34 stubs in total, see Supplementary material, Table S1). Although the CPDM units were running for the entire shift (i.e., between 8 and 10 hr), which is standard practice based on the way the units are programmed for regulatory monitoring, they were kept inside a transport case to limit dust collection except while set up in the target sampling locations (i.e., generally about 3.6 to 5.4 hr, or about 40 to 80% of the entire shift length). When the sampling team arrived at a target location, they set up one or two CPDM units along with three CMDPSUs to collect the paired PVC filter samples; across all 20 events, this yielded 34 CPDM stubs and 72 filter samples. Each CMDPSU used the same 10 mm Dorr-Oliver cyclone, air pump, and flow rate stated above to collect respirable dust directly onto a pre-weighed 37 mm PVC filter. In each location, the CPDMs and paired CMDPSUs were all hung from a steel frame at a height of approximately 1.5 to 2.0 m with the sampling inlets oriented in the same direction, and they were all allowed to sample for the same duration. When the CMDPSUs were stopped, the CPDMs were placed back inside the transport case until they were stopped at the end of the shift.

Sample preparation

Following each shift, each CPDM stub was carefully removed from the CPDM unit and placed into a clean, 50 mL PP test tube for transport. Then, the CPDM's data log was downloaded. Each unit's internal tapered element oscillating microbalance (TEOM) determines the accumulated dust mass on the filter per minute, which is used to report the mass after applying a correction bias (for internal dust loss and thermal zero drift), and then converts the mass on an MRE-equivalent basis[1]) using a multiplier (Volkwein et al. 2006; Page et al. 2007, 2008). This data and the corrections were used to estimate the mass collected over the entire shift and the mass collected in the target location per Equation 2:

$$M_{CPDM} = \frac{(M_2 - M_1)\left(1 + \frac{6.6}{100}\right)}{1.05} - 0.0255 \qquad (2)$$

where, M_1 and M_2 are the CPDM-recorded mass (mg) at the start and end times of the relevant sampling period (i.e., shift or target location), respectively, 6.6% is the internal dust loss correction bias, 0.0255 is the thermal zero drift bias correction (mg), and 1.05 is the MRE conversion factor. To recover dust from each CPDM stub and deposit it for FTIR analysis (i.e., onto a pre-weighed 25 mm PVC filter) the same procedures described above for blank CPDM samples were used. In total, 24 of the field CPDM stubs were recovered in IPA and the other 10 were recovered in H_2O. After the 25 mm PVC filters deposited with dust were dry, they were re-weighed, and the total sample mass was determined using Equation 1.

The reference field samples collected directly onto pre-weighed 37 mm PVC filters (i.e., using CMDPSUs) were kept in their original cassettes for transport back to the laboratory. There, they were re-weighed and the total sample mass for these filters was also determined per Equation 1.

FTIR analysis

Analysis of samples prepared from CPDM filter stubs

All 25 mm PVC filter samples prepared from the blank, spiked, and field CPDM stubs were analyzed by FTIR to estimate quartz mass. For this, an Alpha II spectrometer and the accompanying OPUS software (Bruker Optics, Billerica, MA) were used. The filter was placed into a custom 3-D printed analysis cassette, which was mounted in the spectrometer chamber using a custom-printed holder (Figure 2). The square cassette and holder have dimensions such that the filter center is aligned with the spectrometer's infrared beam (6 mm

Figure 2. 3-D printed 25 mm cassette holder (left) shown with the square cassette (right).

diameter). Based on the prior work to establish optimal scanning locations for 25 mm filter samples yielded by the dust deposition procedure used here (Greth and Sarver 2025), a spacer bar was placed under the cassette such that the beam was offset from the filter center by a distance of 8 mm. Then, the filter was scanned at four 8 mm offset locations (90° apart) by simply rotating the cassette.

The filter samples were prepared from CPDM stubs and analyzed in batches. To initiate analysis of each batch, a blank PVC filter was scanned at its center (i.e., using the cassette and holder shown in Figure 2 with no spacer bar), and the resulting spectrum was used for a blank correction to account for any background interference from the PVC media itself or environmental conditions (e.g., humidity). Each filter sample was analyzed three times on three separate days (events). Since the filter was placed into and removed from the analysis cassette for each event, the actual scan locations varied (i.e., due to the relative rotation of the filter within the cassette).

For each event, the PVC-blank corrected spectrum from each of the four scan locations was used to obtain the integrated spectral peak areas in two predetermined ranges: from 767 cm^{-1} to 816 cm^{-1} cover the unique quartz doublet peak, and from 900 cm^{-1} to 930 cm^{-1} cover the primary kaolinite peak (National Institute for Occupational Safety and Health 2022). Notably, kaolinite is known to commonly occur in respirable coal mine dust samples (Ojima 2003; Miller et al. 2012) and it has a secondary peak that overlaps with the quartz doublet peak, which can cause interference with quartz quantification. However, because the primary and secondary kaolinite peaks occur in near constant ratio, the primary kaolinite peak can be used to correct the secondary peak's interference with quartz per Equation 3:

$$\mathrm{QPA} = \mathrm{QPA}_{\mathrm{uncorrected}} - \frac{\mathrm{KPA}}{3.8} \quad (3)$$

where $QPA_{uncorrected}$ is the integrated area under the quartz doublet peak (arbitrary units); KPA is the integrated area under the primary kaolinite peak (arbitrary units); 3.8 is the constant ratio between the primary and secondary kaolinite peaks; and QPA is the kaolinite-corrected quartz peak area (arbitrary units) (Pokhrel et al. 2022).

For each event, the QPA values were then averaged (i.e., across all four scan locations) and used to predict the quartz mass on the sample filter (Q_{pred}, mg) per Equation 4:

$$Q_{pred} = \frac{QPA}{f} \quad (4)$$

where f is a QPA-to-quartz mass calibration factor. For the specific dust deposition (i.e., 25 mm PVC filter using an inline PP syringe filter holder) and scanning locations used here (i.e., four points at 8 mm offset from center), the previous work by Greth and Sarver (2025) established this factor to be 7.48.

Finally, the Q_{pred} values from each event were averaged to obtain a mean value and standard deviation for each sample.

Analysis of reference field samples

FTIR analysis was also conducted on the reference field samples collected by CMDPSUs. For these samples, the FTIR analysis was done directly on the 37 mm PVC filter per the method standardized by National Institute for Occupational Safety and Health (2022). Each filter was placed into an analysis cassette and holder designed to align the center of a 37 mm filter with the spectrometer beam, and a single scan was performed on the filter center. Again, the resulting spectrum was PVC-blank corrected, and the integrated quartz and primary kaolinite peak areas were used to determine "QPA" per Equation 3.

Equation 4 was again used to predict quartz mass from "QPA" for the reference samples. This time, however, the calibration factor (f=12.3) was established using a linear regression model of "QPA" *vs.* quartz mass determined by the standard NIOSH Method 7603 for 10 (of 72 total) reference samples (The Method 7603 analysis was performed by a contract lab, and the calibration curve is shown in Supplementary material, Figure S1.).

Data analysis

The results from the blank CPDM samples were used to evaluate the range of total mass and quartz mass that might be associated with the CPDM dust recovery and redeposition procedures used here; and to establish corrections (i.e., based on median observed values as discussed below). After applying those corrections, the predicted quartz mass values for the spiked and field CPDM samples were compared to expected values, computed using Equation 5:

$$Q_{\mathrm{exp}} = M * P_Q \quad (5)$$

where M is total sample mass (per Equation 1) and P_Q is the percent quartz in the sample. For the CPDM samples spiked with respirable dust from the bolter dust or roof rock material, P_Q was taken as 9.51% or 10.5%, respectively; as noted above, these values were previously determined and reported by Greth and

Sarver (2025). For each of the field CPDM samples, P_Q was estimated as the average value observed for the three paired reference samples (i.e., using the ratio of predicted quartz mass per Equation 4 and total sample mass per Equation 1 for the 37 mm PVC filters analyzed direct-on-filter).

Results and discussion

Blank CPDM samples

Data for the blank CPDM samples are tabulated in the Supplementary material. Tables S2 and S3 (Supplementary material) show for the samples recovered in IPA and H_2O, respectively, the total sample mass (per Equation 1), corrected quartz peak area (per Equation 3) for each FTIR scan location per analysis event and mean predicted quartz mass (per Equation 4). Figure 3 plots the mean predicted quartz mass as a function of the total sample mass, and linear regression trendlines and their equations are shown (Notably, one sample recovered in IPA [blank CPDM sample S14] was identified as an outlier using the "greater than 1.5× outside than the interquartile range" rule and was removed from the plot and the regression analysis.).

Figure 3 shows that, regardless of whether IPA or H_2O was used as the recovery liquid, the total sample mass—presumably due to residue from the CPDM stub—was limited to about 0.040 mg. However, while the H_2O recovery yielded consistently low values of mean predicted quartz mass (i.e., between about 0.005–0.012 mg for all 20 samples), the IPA recovery occasionally yielded higher values (i.e., >0.012 mg for 5 of 20 samples). This suggests the IPA recovery can sometimes promote either higher removal of quartz-containing residue from the CPDM stub or more efficient transfer of that residue to the PVC filter for analysis. There is also potential that unevaporated IPA is interfering with quartz determination despite waiting a day after deposition to analyze the samples (Ainsworth 2005). Anecdotally, during the recovery procedure, it was observed that the CPDM stub sinks in IPA, but floats in H_2O. This is consistent with differences in the density of the two liquids (i.e., IPA is less dense than H_2O)—and likely increased the contact between the IPA and the stub surfaces *vs.* the H_2O. Further, the relatively lower surface tension of IPA probably results in better transfer of particulates because they should be less likely to stick to the recovery tube and syringe surfaces (Mizerski 2018; Zdziennicka and Jańczuk 2020).

In an unknown sample prepared from a CPDM stub, there will be no way to differentiate between the mass contributed by the stub itself (i.e., residue) *vs.* the dust. To account for any residue, the data shown in Figure 3 were used to establish corrections for both total sample mass, predicted quartz mass, and recovery efficiency per Equations 6 and 7:

$$M' = M - M_{blank} \tag{6}$$

$$Q_{pred}{}' = Q_{pred} - Q_{pred\_blank} \tag{7}$$

where M′ and $Q_{pred}{}'$ are the blank stub-corrected total sample mass (mg) and predicted quartz mass (mg), respectively, and M_{blank} and Q_{pred_blank} are the median total sample mass and predicted quartz mass values observed for the CPDM blank samples. For the H_2O recovery ($n = 20$), M_{blank} was 0.014 mg and Q_{pred_blank} was 0.009 mg; for the IPA samples ($n = 19$), M_{blank} was 0.025 mg and Q_{pred_blank} 0.010 mg.

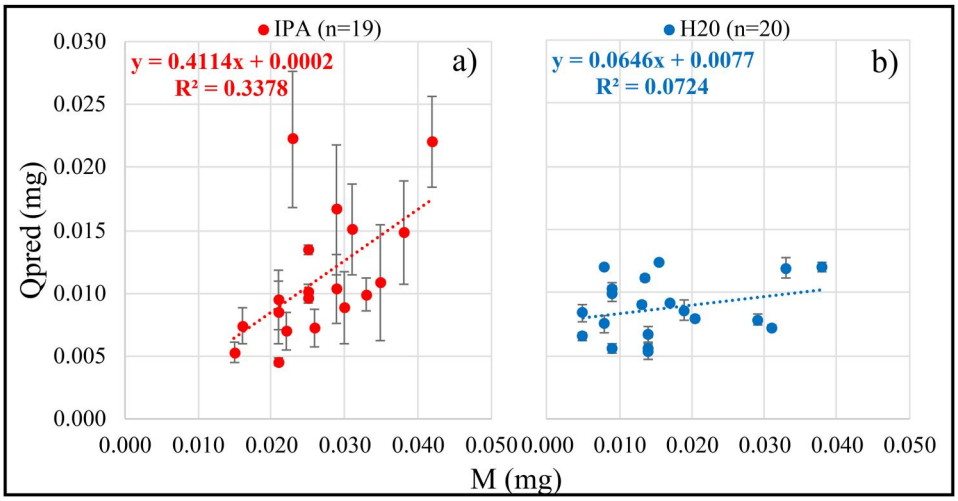

Figure 3. Mean predicted quartz mass *vs.* total sample mass for blank CPDM stubs recovered in (a) IPA and (b) H_2O. Error bars indicate the standard deviation from the mean for predicted quartz mass (i.e., across all three analysis events).

Spiked CPDM samples

Data for the CPDM samples spiked with either bolter dust or roof rock are given in Tables S4 and S5 (Supplementary material), respectively, including the total sample mass (per Equation 1) and corrected total sample mass (Equation 6); kaolinite-corrected quartz peak area (Equation 3) for each FTIR scan location per analysis event; and mean predicted quartz mass (Equation 4) and corrected predicted quartz mass (Equation 7). Figure 4 plots the mean predicted quartz mass against the expected quartz mass for these samples, again with results from the IPA and H_2O recovery liquids shown separately. In Figure 4, the results are presented with and without the blank CPDM-stub corrections for comparison (Notably, the Equation 6 correction for quartz mass affects the Q_{pred} value directly, and the Equation 7 correction for total sample mass affects the Q_{exp} value per Equation 5.).

Figure 4 shows a strong correlation between predicted and expected quartz mass, with both the corrected and uncorrected results exhibiting R2 values >0.97 regardless of the recovery liquid. (Notable differences were not observed between the two dust types used to spike the samples.) Since the blank CPDM-stub corrections are relatively small concerning the total sample mass and predicted quartz mass for most samples, the regression line equations are quite similar for uncorrected and corrected data, with the main difference being reduced y-intercept values for the corrected data. In essence, these values indicate that, for a sample with no quartz content, the FTIR analysis (including blank CPDM-stub correction) would yield a predicted quartz mass of about 0.002 mg for IPA recovery or about 0.001 mg for H_2O recovery. The regression line slopes (i.e., about 0.86 for IPA and 0.85 for H_2O) indicate a tendency to underpredict quartz mass; and close inspection of the data shows that this tendency increases as the quartz mass on the filter increases. This trend is likely an effect of total sample mass—which is about 10× the expected quartz mass for the spiked CPDM based on the quartz content in the dust (i.e., 9.51 or 10.5%). As discussed in the prior work by Greth and Sarver (2025), with increasing total sample mass, the dust deposition pattern on the 25 mm PVC filter may change slightly (i.e., to become more center-heavy). It is also possible that higher-mass samples are more susceptible to mass loss during handling—though the narrow error bars shown in Figure 4 (for all but one sample prepared in IPA) indicate little event-to-event variation.

Overall, the results shown in Figure 4 are consistent with those of the prior work by Greth and Sarver (2025): using the same coal mine source materials to create respirable dust suspensions in IPA (but without a blank CPDM stub), the same procedure and syringe filter apparatus to deposit the dust onto 25 mm PVC filters, and the same FTIR scanning pattern and *QPA*-to-quartz mass calibration factor, the correlation between predicted and expected quartz mass had an R^2 value of 0.91, and the linear regression line equation had a y-intercept of 0.006 mg and a slope of 0.94.

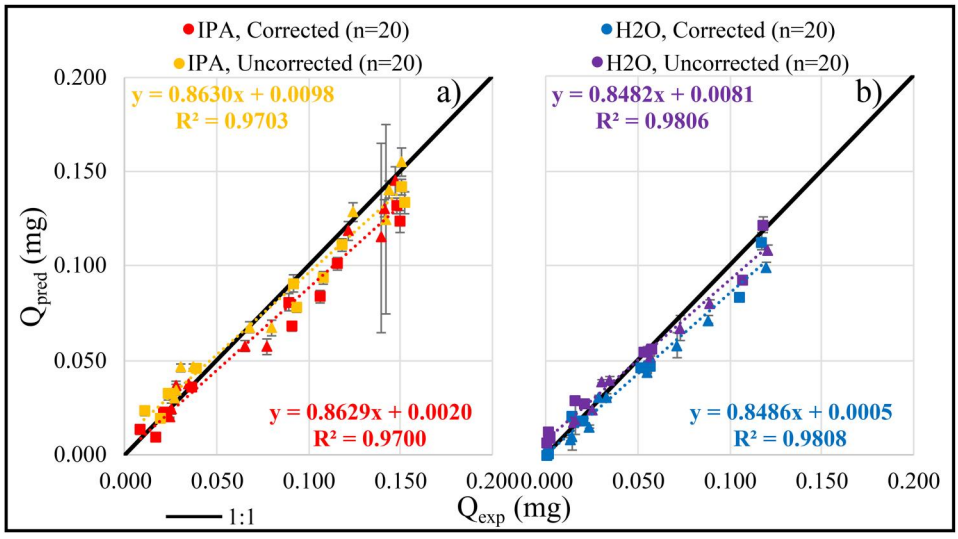

Figure 4. Mean predicted quartz mass *vs.* expected quartz mass for spiked CPDM samples prepared in (a) IPA and (b) H_2O recovery. A 1:1 line is shown for reference. On both plots, results are shown with and without total sample mass and quartz mass corrections to account for blank CPDM-stub residue. Error bars indicate the standard deviation from the mean for predicted quartz mass (i.e., across three analysis events). Samples spiked with bolter dust material and roof rock material are represented by squares and triangles, respectively.

To evaluate the accuracy of predicted quartz mass values against the expected values for the spiked CPDM samples, root mean square error (RMSE) was computed. For the samples prepared in IPA, RMSE was 0.014 and 0.010 mg for corrected and uncorrected data, respectively; and for the samples prepared in H_2O, the RMSE values were 0.010 and 0.008 mg. The relatively higher RMSE values associated with the corrected data are again due to results on higher-mass samples, for which the quartz mass is already being somewhat underpredicted (i.e., per Figure 4). This highlights that, while the blank CPDM-stub correction is particularly important for lower-mass samples, the effect of (what appears to be) gradually changing deposition pattern with total sample mass becomes more relevant for higher-mass samples.

Field samples

For the field CPDM samples, the relative efficiency of transferring the dust mass from the CPDM stub to the 25 mm PVC filter for analysis was evaluated. For this, recovery efficiency (R') was estimated using Equation 8:

$$R' = \frac{M'}{M_{CPDM}} * 100\% \quad (8)$$

where M' and M_{CPDM} are determined per Equations 6 and 2, respectively. Note that M' was used rather than M since the recovery efficiency should account for the blank-stub correction to the total sample mass analyzed by FTIR.

Data for the field CPDM samples are given in Table S6 (Supplementary material), including the total sample mass (per Equation 1) corrected total sample mass (Equation 6); estimated dust recovery efficiency (Equation 8); kaolinite-corrected quartz peak area (Equation 3) for each FTIR scan location per analysis event; and mean predicted quartz mass (Equation 4) and corrected predicted quartz mass (Equation 7). Table S7 (Supplementary material) gives the results for the three paired reference samples collected alongside each of the field CPDM stubs, including the total sample mass (per Equation 1) and predicted quartz mass (per Equation 4). For context, the estimated range of quartz percentage for the field samples was 1.86-11.0% based on the ratio of predicted quartz mass to total sample mass for the reference samples.

Figure 5 shows the distribution of estimated recovery efficiency values for the field CPDM samples prepared using IPA ($n = 24$) and H_2O ($n = 10$), as well as the recovery efficiency *vs.* total CPDM stub sample mass (i.e., per Equation 2 using the entire sampling duration). Removal of dust from the stub and transfer to the 25 mm PVC filter for FTIR analysis was much more efficient using IPA (mean of 55.7%) *vs.* H_2O (mean of 15.8%); and a Student's t-test (at 95% confidence, assuming unequal variance) confirmed the difference is statistically significant ($p < 0.01$). The enhanced recovery efficiency in IPA is attributed to the increased contact between the liquid and the CPDM stub's filter area, and improved dispersion of particles within the suspension (per the previous discussion). Interestingly, no correlation was observed between recovery efficiency and total CPDM stub sample mass. Indeed, efficiency was estimated to be 50% or greater for 18 (of 24 total) CPDM stubs recovered in IPA, including all stubs with less than 1.000 mg of total mass. For the six stubs exhibiting lower recovery efficiency (<50%), it is possible that some of the dust mass was lost during handling of the stub (i.e., during removal from the CPDM unit following mine sampling, or transfer between the test

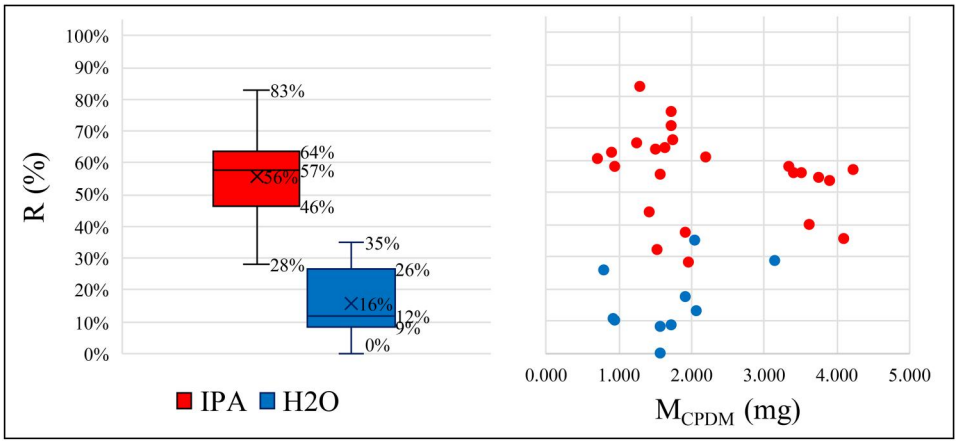

Figure 5. Recovery efficiency observed for field CPDM samples prepared in IPA and H_2O. Plot (a) shows the overall distribution of values and (b) shows blank stub-corrected recovery efficiency *vs.* total dust mass collected on the CPDM stub.

tube used to transport the sample and tube used for the recovery procedure.) For the 10 CPDM stubs recovered in H_2O, there was similarly no correlation between recovery efficiency and total sample mass on the stub—but only three samples exhibited an efficiency greater than 25%. For practical applications, such low values may not support meaningful quartz mass predictions.

Figure 6 shows the mean predicted quartz mass against the expected quartz mass for the field CPDM samples. (No samples were identified as outliers.) For the samples prepared in H_2O, the results indicated very good agreement between the predicted and expected values—especially for the data considering the blank CPDM-stub correction, which yielded a regression line with a low y-intercept (0.007 mg) and nearly ideal slope (0.98). That said, the relatively low recovery efficiency in H_2O is evident, with all samples expected to have less than 0.050 mg of quartz mass (and total sample masses less than about 1.000 mg, see Supplementary material, Table S6).

For the samples prepared in IPA, Figure 6 illustrates that the higher recovery efficiency yielded a wider distribution of quartz mass values (i.e., up to about 0.225 mg, with total sample masses up to about 2.400 mg). As observed for the spiked CPDM samples, there is an apparent tendency to underpredict quartz mass; but the slope of the regression lines for the field CPDM samples in Figure 6a (i.e., about 0.63 *vs.* 0.86 for the spiked CPDM samples) suggests the underprediction is more severe. Again, there may be an effect of total sample mass (i.e., quartz mass values appear to be substantially underpredicted for higher mass samples), however, additional factors might also be at play which are related to the paired reference samples (i.e., used to estimate expected quartz mass for each of the CPDM samples).

One such factor could be the different sampling times for the CPDMs and reference samples: As described earlier, the reference samples were collected in the target sampling locations alongside the CPDM stubs. However, though the CPDMs collected most of the total stub mass in the target location (i.e., mean of 80% per data in Supplementary material, Table S1), they collected some of the mass during the preceding and subsequent time intervals (i.e., which made up the balance of the full shift duration). Since the dust collected in the target locations is generally expected to have higher quartz content than dust collected during other time intervals (e.g., transport in an out of the mine), some CPDM samples were likely diluted in effect—meaning their quartz mass values should be somewhat lower than the expected values derived from the reference samples. This could contribute to the relatively low slope of the regression lines in Figure 6a.

Another factor affecting the apparent underprediction of quartz mass from the field CPDM samples could be the accuracy of the direct-on-filter FTIR analysis on the reference samples: As explained earlier, this analysis was used to derive the mean expected quartz mass values shown in Figure 6a (i.e., by predicting quartz mass on triplicate reference samples such that quartz percentage in the sampling location

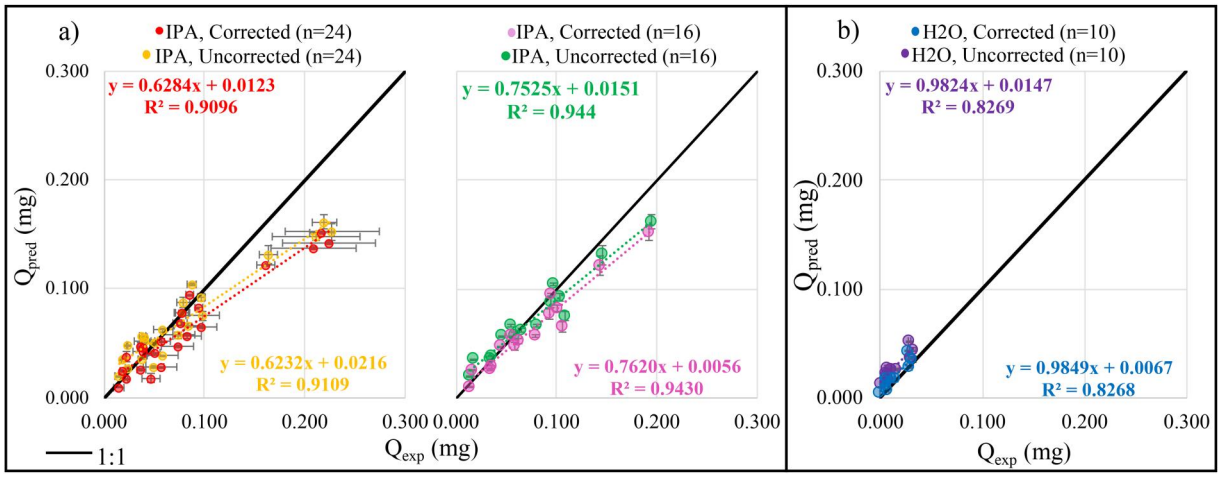

Figure 6. Mean predicted quartz mass *vs.* expected quartz mass for field CPDM samples prepared in (a) IPA and (b) H20. To determine expected quartz mass (per Equation 5), the left plot in (a) and the plot in (b) used direct-on-filter FTIR analysis of the reference samples to estimate percent quartz); however, the right plot in (a) uses results derived from Method NIOSH 7603 analysis. A 1:1 line is shown for reference. On both plots, results are shown with and without total sample mass and quartz mass corrections to account for blank CPDM-stub residue. Error bars indicate the standard deviation from the mean for predicted quartz mass (i.e., across three analysis events) and expected quartz mass values (i.e., across three reference samples).

could be estimated). However, the wide error bars on many of the expected quartz mass values in Figure 6a indicate substantial uncertainty. Although differences between triplicate reference samples could simply indicate spatial variability in the sampling location, this would not explain the consistent and substantial negative bias for quartz mass predicted from the paired CPDM samples. More likely, the dust loading pattern on the reference sample filters was somewhat variable, which would effectively change the relationship between observed QPA and quartz mass. In high-concentration environments, respirable dust loading on filters (collected with the same CMDPSUs used here) tends to be center-heavy (Pokhrel et al. 2021; Keles et al. 2022); and using a single center-point scan for FTIR analysis should cause overestimation of quartz mass. To interrogate this possibility, Figure 6b shows the predicted quartz mass for the field CPDM samples that had a paired reference sample analyzed by NIOSH Method 7603 ($n = 16$); for these data points, the expected quartz mass is based on the Method 7603 result, which should not be affected by deposition pattern. The increased slope of the trendline (i.e., 0.76 using Method 7603-derived expected quartz mass) supports the idea that the direct-on-filter FTIR analysis likely overestimated the quartz mass on some reference filters—especially those with higher total sample mass.

In summary, it appears that the field CPDM samples results shown in Figure 6 are affected by both the underprediction of quartz mass on the recovered 25 mm filter, and the overestimation of the expected quartz mass derived from the paired reference samples. Combined, these factors help explain the relative difference trends between the spiked CPDM sample results shown in Figure 4 and the field CPDM sample results shown in Figure 6.

Study implications and limitations

This study aimed to evaluate a method enabling the determination of quartz (as a surrogate for RCS) in dust samples collected using CPDMs, such that RCS monitoring efforts in coal mines can be expanded simply by leveraging CPDM samples that are already being collected. The method studied here essentially requires that dust can be efficiently recovered from the CPDM stub and redeposited onto a PVC filter; FTIR analysis can be conducted to predict the quartz mass on that filter; and corrections can be made to account for any interference yielded by residue recovered from the stub itself.

Regarding dust recovery, the field CPDM samples demonstrated that IPA may be a viable liquid, but more work is needed to address the range of recovery efficiency values that might be achieved. Here, IPA recovery typically yielded values >50% (i.e., for 18 of 24 CPDM stubs), but six values were below this threshold range (ranging between 28 and 44%). High recovery efficiency is needed to ensure adequate dust to exceed limits of detection (LOD) and quantification (LOQ) thresholds, which were previously determined to be around 0.005 and 0.018 mg for blank PVC media (see Greth and Sarver 2025)—and will increase when considering the possibility of CPDM-stub residue (see below). However, for a field-based method, a narrow range of expected recovery efficiency is also important for the interpretation of results. This is because, without a sensitive microbalance, the total mass of the recovered sample probably cannot be determined, so reporting quartz mass or mass concentration in the original CPDM requires some assumption of recovery efficiency. As an example, suppose a CPDM stub collected dust over an 8-hr shift (at the standard 2.2 L/min flowrate), and the predicted quartz mass on the recovered sample (i.e., on a 25 mm PVC filter) was 0.100 mg. Using the high (83%) and low end (28%) of the range of IPA recovery efficiency observed here, the quartz mass on the CPDM stub could be reported as being between 0.028 and 0.083 mg, and yielding a mass concentration between 26 and 79 $\mu g/m^3$. With a narrower range of expected recovery efficiency, the results could be reported more precisely. That said, given the sheer number of CPDM samples being collected in mines and the relative simplicity of the proposed dust recovery and analysis method, a method such as the one evaluated here could be performed in a centralized lab with capabilities to directly determine the recovered dust mass.

Regarding the prediction of quartz mass on the recovered sample filter, results presented here suggest the deposition pattern on the filter may gradually change with total sample mass—yielding increasingly underpredicted values. This was observed for both the spiked and field CPDM samples, however, the field sample results should be viewed with ample caution considering the likely issues surrounding their paired reference samples (i.e., which affected the regression lines shown in Figure 6). For the spiked CPDM samples, the results shown in Figure 4 (for IPA recovery) suggest the under-prediction should only be about 12% for a sample with 1.500 mg of total dust with 10% quartz content; and, to reiterate, this fits well with findings in the prior work to develop the dust

deposition and FTIR analysis procedures (Greth and Sarver 2025) Nevertheless, if relatively larger sample sizes are expected, this problem could be addressed by considering multiple QPA-to-quartz mass calibration factors, or other PVC filter sizes and/or deposition apparatus designs.

Regarding the possibility of residue from the CPDM stub itself, results here suggest that the associated quartz mass is typically small (i.e., less than 0.012 mg)—however, the IPA recovery can sporadically yield higher values. This affected the numerical correction (i.e., established as 0.010 mg quartz mass), and will also affect the uncertainty of the results. For direct-on-filter FTIR analysis of quartz in dust samples, LOD and LOQ have been reported considering the standard deviation of results observed on blank PVC filters; specifically, LOD and LOQ were determined as 3× and 10× standard deviation, respectively (e.g., see Lorberau 1990; Farcas et al. 2016). This approach was also taken in the prior work to establish the dust deposition and FTIR analysis procedures used here (Greth and Sarver 2025) However, for samples recovered from CPDM stubs, determination of LOD and LOQ could consider "procedural blank PVC filters," meaning filters that have been prepared using blank CPDM stubs to account for the residue they contribute to the final sample. Using the data shown in Figure 3, this approach would yield an LOD of 0.019 mg and LOQ of 0.062 mg, which are much higher than desired—especially given the PEL and action level set by the "new silica rule." To address this issue, more work is required to evaluate the recovery procedure used here, or modifications of it. In particular, it is necessary to determine if or how handling of the CPDM stub may affect the total residue mass and its quartz content, and the rate of high quartz-mass residue observations for different batches of CPDM stubs. Such work may narrow the range of quartz mass associated with the blank stubs, and thereby lower the LOD and LOQ values.

Conclusions

CPDMs are frequently used in US underground coal mines to monitor RCMD. While these instruments cannot directly measure RCS, capabilities for post-hoc analysis of the sample collected by the CPDM could be quite valuable. The method tested here includes three essential steps to (1) recover the dust from the CPDM filter stub, (2) redeposit it to a PVC filter, and (3) analyze that filter by FTIR to predict quartz mass (i.e., as a surrogate for RCS). Results demonstrate that recovery efficiency in IPA can be high (mean of 55.7%), whereas the efficiency in H_2O is much lower (mean of 15.8%). For a field-based method, IPA recovery appears promising, but work is needed to tighten the range of recovery efficiency to enable reporting of quartz mass or mass concentration within the context of the original CPDM sample. Otherwise, the method would need to be performed in a laboratory where the recovered sample mass can be accurately measured. Additional work is also needed to reduce the potential for sporadically high quartz-mass contributions from the CPDM stub itself. Otherwise, the LOD and LOQ of the method tested here will be relatively high, limiting its practicality for real CPDM samples. Finally, the effect of the total recovered sample mass on the predicted quartz mass should be further explored. For the spiked CPDM samples, predicted quartz mass showed a better correlation to the expected quartz masses as indicated by the regression line's slope of 0.86, but for the results for the FIELD CPDMs yield a slope of 0.63 for the regression line. Results in the current study suggest the deposition pattern on the recovered filter might gradually change with increasing mass, and this can affect predicted quartz mass since FTIR analysis is performed on a limited number of locations with results extrapolated across the entire filter. A simple solution might be specific QPA-to-quartz mass calibration factors for samples expected to have "low" *vs.* "high" total recovered sample mass (i.e., based on the CPDM-recorded dust mass and an expected range of recovery efficiency).

Notes

1. The CPDM was designed for regulatory monitoring in US coal mines, where respirable dust exposure standards have historically been based on 'MRE equivalent' mass. This refers to the mass collected by a Mining Research Establishment (MRE) sampler, which yields a slightly different size distribution than the CPDM (and CMDPSU) (Tomb et al. 1973). To account for the effect on sample mass, the CPDM applies a constant MRE equivalency of 1.05 (Page et al. 2008).

Disclosure statement

No potential conflict of interest was reported by the author(s).

Funding

This work was supported by various mine partners who provided the coal mine source materials used in this study and allowed the authors access to their sites for field sampling using their CPDMs. This work was funded by

National Institute for Occupational Safety and Health (NIOSH) [contract 75D30119C05529].

Data availability statement

The authors confirm that the data supporting the findings of this study are available within the article and its supplementary materials.

References

Agioutanti E, Keles C, Sarver E. 2020. A thermogravimetric analysis application to determine coal, carbonate, and non-carbonate minerals mass fractions in respirable mine dust. J Occup Environ Hyg. 17(2-3):47–58. doi: 10.1080/15459624.2019.1695057.

Ainsworth SM. 2005. Infrared analysis of respirable coal mine dust for quartz: thirty five years. J. ASTM Int. 2(4): 1–13. doi: 10.1520/JAI12231.

Blackley DJ, Halldin CN, Laney AS. 2018. Continued increase in prevalence of coal workers' pneumoconiosis in the United States, 1970-2017. Am J Public Health. 108(9):1220–1222. doi: 10.2105/AJPH.2018.304517.

Chow JC, Watson JG, Wang X, Abbasi B, Reed WR, Parks D. 2022. Review of filters for air sampling and chemical analysis in mining workplaces. Minerals. 12(10):1314. doi: 10.3390/min12101314.

Cohen RA, Rose CS, Go LHT, Zell-Baran LM, Almberg KS, Sarver EA, Lowers HA, Iwaniuk C, Clingerman SM, Richardson DL, et al. 2022. Pathology and mineralogy demonstrate respirable crystalline silica Is a Major Cause of Severe Pneumoconiosis in U.S. Coal Miners. Ann Am Thorac Soc. 19(9):1469–1478. doi: 10.1513/AnnalsATS.202109-1064OC.

Elie G, Pandey R, Sarver EA. 2024. Direct-on-filter FTIR analysis of respirable crystalline silica: a field study to demonstrate utility for routine non-regulatory monitoring in coal mines. Mining Metall. Explor. 41(6):2833–2834. doi: 10.1007/s42461-024-01160-6.

Farcas D, Lee T, Chisholm WP, Soo JC, Harper M. 2016. Replacement of filters for respirable quartz measurement in coal mine dust by infrared spectroscopy. J Occup Environ Hyg. 13(2):D16–D22. doi: 10.1080/15459624.2015.1091962.

Goldberg S, Tomb T, Kacsmar P, Baber J, Busa M. 1984. MSHA's procedure for determining quartz content of respirable coal mine dust. Informational report. Pittsburgh (PA): Mine Safety and Health Administration, U.S. Department of Labor. Report No.: IR 1152.

Greth A, Sarver E. 2025. Toward rapid silica analysis of CPDM samples: deposition of recovered dust and analysis by FTIR. J Occup Environ Hyg. 22(2):87–100. doi: 10.1080/15459624.2024.2421008.

Hall NB, Blackley DJ, Halldin CN, Laney AS. 2019. Current review of pneumoconiosis among US coal miners. Curr Environ Health Rep. 6(3):137–147. doi: 10.1007/s40572-019-00237-5.

Hall NB, Halldin CN, Blackley DJ, Laney AS. 2020. Assessment of pneumoconiosis in surface coal miners after implementation of a national radiographic surveillance program, United States, 2014–2019. Am J Ind Med. 63(12): 1104–1108. doi: 10.1002/ajim.23184.

Harris DA, Almberg KS, Blackley DJ, Cohen RA, Edwards C, Johnson B, Hall NB. 2024. Progressive massive fibrosis identified at federally funded black lung clinics in the US. JAMA. 331(5):438–440. doi: 10.1001/jama.2023.25578.

Infrared determination of quartz in respirable coal mine dust (U.S.). 2013. Mine Safety and Health Administration (MSHA), US Department of Labor. Report No.: P-7.

Keles C, Pokhrel N, Sarver E. 2022. A study of respirable silica in underground coal mines: sources. Minerals. 12(9):1115. doi: 10.3390/min12091115.

Key-Schwartz RJ, Baron PA, Bartley DL, Rice FL, Schlecht PC. 2003. Determination of airborne crystalline silica. In: NIOSH manual of analytical methods. 4th ed., 3rd Suppl. Cincinnati (OH): U.S. Department of Health and Human Services, Public Health Service, Centers for Disease Control and Prevention, National Institute for Occupational Safety and Health, DHHS(NIOSH) Publication No. 2003–154.

Lorberau C. 1990. Technical brief: investigation of the determination of respirable quartz on filter media using Fourier transform infrared spectrophotometry. Appl Occup Environ Hyg. 5(6):348–350. doi: 10.1080/1047322X.1990.10389652.

Lowering miners' exposure to respirable coal mine dust, including continuous personal dust monitors. 2014. Mine Safety and Health Administration (MSHA). US Department of Labor. Document No.: 2019-09084.

Lowering miners' exposure to respirable crystalline silica and improving respiratory protection. 2024. Mine Safety and Health Administration (MSHA). US Department of Labor. Document No.: 89 FR 44852.

Miller AL, Drake PL, Murphy NC, Noll JD, Volkwein JC. 2012. Evaluating portable infrared spectrometers for measuring the silica content of coal dust. J Environ Monit. 14(1):48–55. doi: 10.1039/c1em10678c.

Miller AL, Murphy NC, Bayman SJ, Briggs ZP, Kilpatrick AD, Quinn CA, Wadas MR, Cauda EG, Griffiths PR. 2015. Evaluation of diffuse reflection infrared spectrometry for end-of-shift measurement of quartz in coal dust samples. J Occup Environ Hyg. 12(7):421–430. doi: 10.1080/15459624.2015.1011328.

Mizerski A. 2018. Wetting properties of aqueous short-chain alcohols' solutions. MATEC Web Conf. 247:00064. doi: 10.1051/matecconf/201824700064.

[NASEM] National Academies of Sciences, Engineering, and Medicine. 2018. Monitoring and sampling approaches to assess underground coal mine dust exposures. Washington (DC): The National Academies Press. doi: 10.17226/25111.

National Institute for Occupational Safety and Health. 2022. Direct-on-filter analysis for respirable crystalline silica using a portable FTIR instrument. Pittsburgh (PA): U.S. Department of Health and Human Services, Centers for Disease Control and Prevention, National Institute for Occupational Safety and Health. Report No.: 2022–108, IC 9533. doi: 10.26616/NIOSHPUB2022108.

Ojima J. 2003. Determining of crystalline silica in respirable dust samples by infrared spectrophotometry in the presence of interferences. J Occup Health. 45(2):94–103. doi: 10.1539/joh.45.94.

Page S, Tuchman D, Vinson R. 2007. Thermally induced filter bias in TEOM mass measurement. J Environ Monit. 9(7):760–767. doi: 10.1039/b704424k.

Page S, Volkwein J, Vinson R, Joy G, Mischler S, Tuchman D, McWilliams L. 2008. Equivalency of a personal dust monitor to the current United States coal mine respirable dust sampler. J Environ Monit. 10(1):96–101. doi: 10.1039/b714381h.

Pokhrel N, Agioutanti E, Keles C, Afrouz S, Sarver E. 2022. Comparison of respirable coal mine dust constituents estimated using FTIR, TGA, and SEM–EDX. Mining Metall Explor. 39(2):291–300. doi: 10.1007/s42461-022-00567-3.

Pokhrel N, Keles C, Jaramillo L, Agioutanti E, Sarver E. 2021. Direct-on-filter FTIR spectroscopy to estimate calcite as a proxy for limestone 'rock dust' in respirable coal mine dust samples. Minerals. 11(9):922. doi: 10.3390/min11090922.

Tomb TF, Treaftis HN, Mundell RL, Parobeck PS. 1973. Comparison of respirable dust concentrations measured with MRE and modified personal gravimetric sampling equipment. Washington, DC: U.S. Department of Interior, Bureau of Mines. RI 7772.

Tuchman DP, Volkwein JC, Vinson RP. 2008. Implementing infrared determination of quartz particulates on novel filters for a prototype dust monitor. J Environ Monit. 10(5):671–678. doi: 10.1039/b803804j.

Vanka KS, Shukla S, Gomez HM, James C, Palanisami T, Williams K, Chambers DC, Britton WJ, Ilic D, Hansbro PM, et al. 2022. Understanding the pathogenesis of occupational coal and silica dust-associated lung disease. Eur Respir Rev. 31(165):210250. doi: 10.1183/16000617.0250-.2021.

Volkwein J, Vinson R, Page S, Joy G, Mischler S, Tuchman D, McWilliams L. 2006. Laboratory and field performance of a personal dust monitor. Pittsburgh, PA: U.S. Department of Health and Human Services, Centers for Disease Control and Prevention, National Institute for Occupational Safety and Health. Report No: RI 9669.

Zdziennicka A, Jańczuk B. 2020. Modification of adsorption, aggregation and wetting properties of surfactants by short chain alcohols. Adv Colloid Interface Sci. 284:102249. doi: 10.1016/j.cis.2020.102249.